Unconventional ferrimagnetic ordering of Ce in the anisotropic metal $CeCrSb_3$

D. D. Jackson and S. K. McCall
Lawrence Livermore National Laboratory, Livermore, California 94550, USA

A. B. Karki and D. P. Young
Louisiana State University, Baton Rouge, Louisiana 70803, USA

(Received 11 May 2007; published 7 August 2007)

We report on the magnetization and electrical resistivity on single crystals of $CeCrSb_3$, a ferromagnetic metal with large anisotropy. It undergoes two ferromagnetic transitions: the first is at $T_{Cr}=115$ K due to the electrons from the Cr ions and the second is a gradual alignment of the Ce^{3+} $4f$ electrons between 48 and 18 K. The Cr moments behave similarly in $LaCrSb_3$, with the easy axis along the b axis. Below 48 K, the Ce moments begin to align along the c axis, and as the applied field increases, their effect on the magnetization increases in importance, resulting in nearly linear behavior of $M_c(T)$ for $H=30$ kG. At 5 K, the saturation moment along the c axis is $3.28\mu_B$/f.u., and along the b axis, the magnetization saturates to $1.29\mu_B$/f.u., the difference being only 7% less than the predicted Hund's rule value for Ce^{3+}, indicating that the $4f$ moments have fully aligned along the c axis.

DOI: 10.1103/PhysRevB.76.064408 PACS number(s): 75.30.Gw, 72.15.−v, 75.20.En

I. INTRODUCTION

The family of compounds $RCrSb_3$ (R=La-Nd, Sm, Gd-Dy, and Yb) displays a variety of magnetic effects due to the interplay between the $3d$ Cr electrons and the $4f$ rare-earth electrons. Its quasi-two-dimensional crystal structure plays an important role in understanding its transport properties. As shown in the inset of Fig. 1, it is a layered system which stacks along the a axis. $CeCrSb_3$ crystallizes in an orthorhombic structure (space group $Pbcm$)[1] with lattice constants of $a=1.311(1)$ nm, $b=0.619(3)$ nm, and $c=0.608(9)$ nm. The crystal structure consists of $CrSb_6$ (distorted) octahedra in the b-c plane, which share faces along the c axis and share edges along the b axis. Separating the stacking of these octahedra is a region of Ce ions and a nearly square sheet of Sb(3). The Ce ions lie above and below this square Sb net in a checkerboardlike arrangement. The strong crystallographic anisotropy will also present itself in the anisotropic transport properties. Bond length considerations suggest that the rare-earth and Cr ions are trivalent, while the Sb, making up the corners of the octahedra, has a valence of −2.5, and the Sb(3) has a valence of −1.[2,3]

The magnetic behavior of the Cr can be isolated by investigating the properties of $LaCrSb_3$, which does not have a $4f$ moment. The crystal structure has only one unique Cr site,[1] yet $LaCrSb_3$ has a rich magnetic phase diagram in which both localized and itinerant spins are present.[4–6] It orders ferromagnetically at $T_{Cr}=132$ K, with the behavior and orientation of the spins dependent on the size of the applied magnetic field. For low fields ($H<0.25$ kG), the spins are oriented along the c axis with small antiferromagnetic canting along the b axis. In addition, for $T<95$ K, the spins rotate within the plane and align along the b axis, with small antiferromagnetic canting along the c axis. The origin of these complex magnetic phases is still in dispute,[7,8] with one possible explanation based on the coexistence of both itinerant and localized moments.[4] For medium strength fields ($0.25<H<3.7$ kG), immediately below T_{Cr}, the quasi-two-dimensional nature of the crystal structure becomes evident with the moments aligning within the b-c plane. However, as the temperature is further reduced, there exists a temperature below which the full magnetic anisotropy becomes evident, and the spins align along the b axis, resulting in a decrease of the magnetization along the c axis. The temperature at which the magnetic anisotropy occurs along each principal axis decreases linearly with the applied field so that for $H>3.7$ kG (the high-field region), the full magnetic anisotropy is suppressed and the Cr moments are found to align in the direction of the magnetic field within the b-c plane.[5]

The crystallographic anisotropy presents itself in the electrical resistivity as well. In this case, band structure calculations show the greatest band overlap along the c axis,[9] which is in the direction of the face-sharing $CrSb_6$ octahedra, and can be pictured as chains of Cr ions (see the upper inset of Fig. 1). Conversely, along the a axis, the band overlap is weakest, suggesting little electrical conductivity between the planes. Electrical resistivity measurements along each axis have confirmed this behavior, showing that the room temperature resistivity along the stacking direction is roughly six times larger than that along the Cr chains. Furthermore, the resistivity is found to be metallic within the b-c plane ($d\rho/dT>0$) for all temperatures below 300 K but insulating ($d\rho/dT<0$) perpendicular to the planes for $T>T_{Cr}$.[5]

The properties of $RCrSb_3$ have also been investigated for R=Ce, Pr, Nd, Sm, Gd, Tb, Dy, and Yb in order to investigate the behavior of increasing the number of localized $4f$ moments. In addition to the ferromagnetic ordering of the Cr moments, the $4f$ moments due to the light rare earths (Ce-Sm) order at a temperature $T<T_{Cr}$.[2,10–12] In contrast, the heavy rare earths (Gd-Dy and Yb) have a single magnetic ordering temperature due to anti-alignment of the Cr and R magnetic sublattices.[3,12–14] The low-field spin-reorientation phase observed in $LaCrSb_3$ is no longer found for these compounds. Otherwise, in the temperature region between the magnetic ordering due to the rare-earth ions and the ordering due to the Cr ($T_R<T<T_{Cr}$), the properties of $RCrSb_3$ are

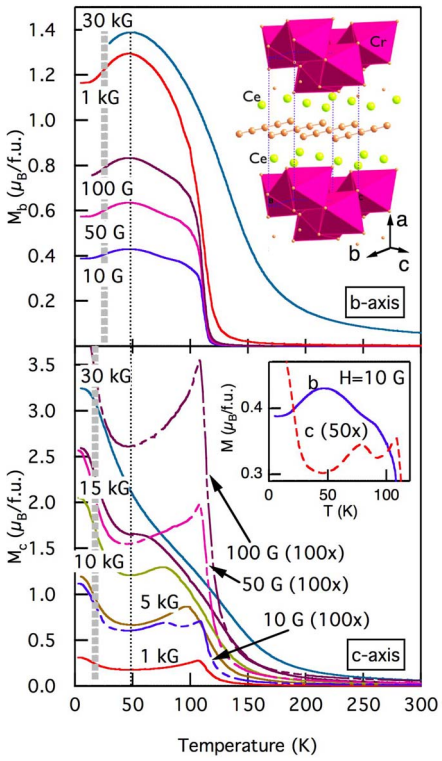

FIG. 1. (Color online) Field cooled magnetization along the *b* axis (top) and *c* axis (bottom) at various fields. In order to see the details for the low-field behavior along the *c* axis, the data for $H=10$, 50, and 100 G (all represented by dashed curves) have been multiplied by a factor of 100. Notice the much larger scale for the *c* axis data. The narrow dashed vertical line at 48 K shows the location of the maximum in M_b and the minimum in M_c. The thick dashed line shows the location of the inflection point at 26 K ($\sim$17 K) for M_b (M_c). The crystal structure for $CeCrSb_3$ is shown in the top inset. The Sb(1) and Sb(2) ions are at the corners of the octahedra, and the Sb(3) make up the nearly square plane in the center of the lattice. The bottom inset shows the *b* axis (solid line) and *c* axis (dashed line, multiplied by 50) magnetizations, highlighting the anomalous features near 85 K that are coincident for both axes.

very similar to the properties of $LaCrSb_3$. Immediately below T_{Cr}, the Cr moments align within the plane and in the direction of the applied field. As the temperature is decreased further, the full anisotropy becomes evident and the Cr spins become oriented along the *b* axis.[10] Using neutron diffraction, Deakin *et al.* found that the Nd moments in $NdCrSb_3$ become ferromagnetic (FM) at 12.7 K, with both the Nd and Cr moments aligned along the *a* axis.[11] Jackson and Fisk investigated $SmCrSb_3$ through magnetization and resistivity measurements and found that this compound is unique in the above-mentioned family of compounds due to its first order ferrimagnetic ordering at 30 K in which the magnetization along the *b* axis discontinuously drops to almost zero, while the resistivity along the *a* axis increases by 77%.[10] Finally, doping studies have been performed on both the Cr site,[15] which shows a small nonlinear effect on the ordering temperature of $LaCrSb_3$, and on the rare-earth site,[16] which shows that the low temperature magnetic phase scales with the de Gennes factor $DG=(g-1)^2J(J+1)$, indicative of the Ruderman-Kittel-Kasuya-Yosida mechanism.[17] In this paper, the magnetic anisotropy of single crystals of $CeCrSb_3$ has been investigated through magnetization and electrical resistivity in order to investigate the effect of trivalent Ce on the properties of $RCrSb_3$.

II. EXPERIMENTAL TECHNIQUE

The procedure for growing single crystals of $RCrSb_3$ has been previously described.[5,10] All measurements were taken on as grown samples. Single phase materials were confirmed using a commercial Scintag powder x-ray diffractometer, and the lattice constants were determined using a Si standard and a least squares fit to a minimum of 20 peaks. Magnetization and magnetic susceptibility measurements were taken with either a commercial superconducting quantum interference device magnetometer (Quantum Design MPMSR2) or a Quantum Design physical property measurement system with the vibrating sample magnetometer option in the temperature range of 2–350 K and $H \leqslant 160$ kG. Electrical resistivity measurements were performed using a standard four-probe technique in the temperature range 5–295 K.

III. RESULTS

Figure 1 shows $M(T)$ for $CeCrSb_3$ with the applied field parallel to the *b* axis (top graph) and *c* axis (bottom graph) at various representative fields. For low fields, the data along the *c* axis were small so the curves at 10, 50, and 100 G have been multiplied by a factor of 100 for clarity. The *a* axis magnetization was not investigated in detail. The Cr electrons order ferromagnetically at $T_{Cr}=115\pm3$ K, which was identified by the intercept of a line through M^2 vs T at 10 G.[18] The large uncertainty is due to the different values obtained along each axis. Arrott plots also indicated a similar value, with similar error due to curvature in the plots at low fields.

Just as in $LaCrSb_3$, the behavior of $CeCrSb_3$ can be described in three different magnetic field ranges. Near zero field ($H \leqslant 20$ G), the magnetization below T_{Cr} initially increased sharply, as expected for a FM transition, and then anomalous behavior was found within the plane at lower temperatures. The lower inset of Fig. 1 shows that M_c (dashed line, multiplied by a factor of 50 for comparison with the *b* axis) has several local maxima and minima. It first increases up to 109 K, then drops to 91 K, and increases again to 78 K before reaching its final minimum at 45 K. Finally, an inflection point in the curvature of M_c was identified by a minimum in dM_c/dT at 16 K. The magnetization along the *b* axis also has structures, with a kink at both 90 and 78 K and a maximum at 47 K. The *b* axis magnetization also displayed an inflection point, in this case at 26 K. These features were observed on two different sample batches and were found at both 10 and 20 G.

The main features of the magnetization for $0.05 \leqslant H < 15$ kG (medium strength fields) begin at $T_{Cr}=115$ K.

Figure 1 shows that M_b has a maximum at 47 K, followed by an inflection point at 26 K, which are both independent of the applied field. The magnetization along the c axis has a local minimum at 48 K and an inflection point at approximately 17 K; both of which are also field independent. For $48\ \mathrm{K} < T < T_{\mathrm{Cr}}$, a local maximum is found in M_c, which decreases as the field increases.

At 15 kG, the local maximum in M_c is located at the same temperature as its local minimum. For $H > 15$ kG, M_b looks very similar to the "medium strength field" region described above, continuing to show a maximum and an inflection point. Along the c axis, the only features are the Curie temperature at T_{Cr} and the inflection point near 17 K. However, the shape of $M_c(T)$ has a unique linear behavior below T_{Cr}, resulting in a magnetization at 2 K along the c axis more than twice of that along the b axis. This behavior is discussed further below.

The magnetic susceptibility ($\chi = M/H$) follows a modified Curie-Weiss law above 200 K, $\chi = \chi_0 + C/(T-\theta)$. The crystallographically averaged results from this give $\chi_0 = 3 \times 10^{-5}$ emu/mol, $C = 1.75$ emu K/mol, and $\theta = 139$ K. Subtracting out the trivalent Curie constant of cerium ($C_{\mathrm{Ce}} = 0.81$ emu K/mol) suggests that Cr has a 4+ valence state, in contrast to the derived Cr^{3+} in $LaCrSb_3$. However, bond length considerations point to a trivalent state for Cr.[1] In addition, various measurements of $LaCrSb_3$, such as specific heat[4] and noninteger saturation moment,[5] all suggest that the Cr moments have itinerant electron behavior which implies that the local moment assumption of a Curie-Weiss analysis to the magnetic susceptibility is unphysical.

Figure 2 shows the strong anisotropy in isothermal magnetization along the b and c axes. At 5 K and 55 kG, M_b saturates to $1.29\mu_B$/f.u., a value only 24% lower than observed for $LaCrSb_3$ at $1.69\mu_B$/f.u. Recall from above that Fig. 1 showed a maximum in M_b at 48 K. This behavior is confirmed here, where $M(T=5\ \mathrm{K}) < M(T=50\ \mathrm{K})$ holds to at least 160 kG, with no anomalous behavior such as a spin-flop transition observed, indicating the strength of the magnetic anisotropy. Along the c axis [Fig. 2(b)], the magnetization is rather different with very little hysteresis, requiring a much larger field to reach its saturation value at 5 K of $3.28\mu_B$/f.u. The difference between these saturation values, $M_c - M_b = 1.99\mu_B$/f.u., is only 7% less than the predicted value of trivalent Ce according to Hund's rules ($2.14\mu_B$). This strongly suggests that at 5 K, the Ce moments are ordered along the c axis. Finally, note that the initial slope of $M_c(H)$ is steeper at 5 K ($0.22\mu_B$/f.u./kG) than it is between 30 and 85 K (roughly $0.12\mu_B$/f.u./kG). The inset of Fig. 2(a) compares the magnetization at 5 K along all three crystallographic axes. This emphasizes the larger magnetization found along the c axis compared to those found along the a and b axes. The behavior of $M_a(H)$ is similar to what was found both in $LaCrSb_3$ (Ref. 5) and in $SmCrSb_3$.[10] In all three of these materials, M_a has not saturated by 55 kG, and $SmCrSb_3$ saturated only after an applied field of 310 kG was applied.[10] The larger magnitude of the a axis magnetization found here for $CeCrSb_3$, compared to that in $LaCrSb_3$, is most likely due to canting of the Ce spins off from the c axis.

The electrical resistivity normalized at 290 K for $CeCrSb_3$ is shown in Fig. 3. Within the b-c plane, the resistivity decreases monotonically with decreasing temperature, in contrast to the a axis resistivity, which is found to initially have $d\rho/dT < 0$. At T_{Cr}, ρ_a reaches a maximum, while ρ_b and ρ_c have a kink in the resistivity plus a peak in $d\rho/dT$ [Fig. 3(a)]. Below T_{Cr}, the resistivity decreases monotonically along each axis until 18 K, where a second peak in $d\rho/dT$ is found.

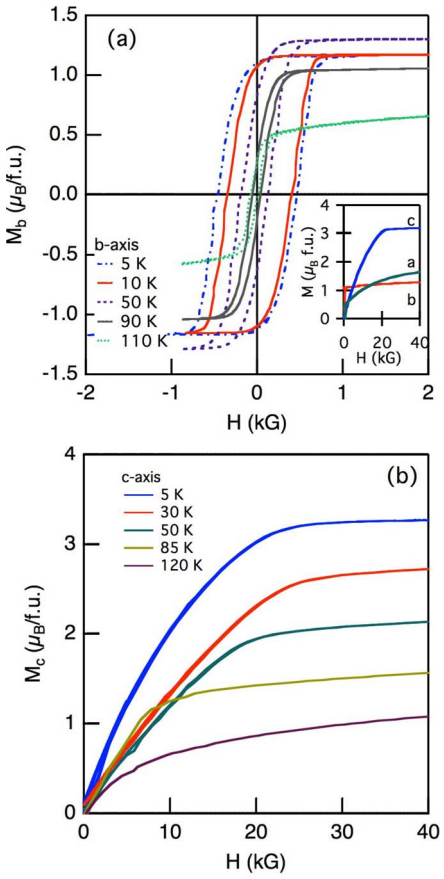

FIG. 2. (Color online) Isothermal magnetization along the (a) b axis and (b) c axis. The inset of (a) shows the magnetization at 5 K for the three principal axes, emphasizing the difference in scale.

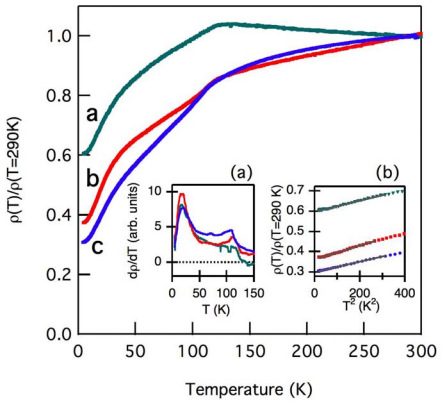

FIG. 3. (Color online) The electrical resistivity normalized at 290 K along each of the principle axis for $CeCrSb_3$. (a) $d\rho/dT$ showing peaks at 115 K due to the Cr ordering and at 18 K, the temperature below which the Ce moments have become fully ordered. (b) ρ vs T^2 up to $T^2 = (20\ \mathrm{K})^2$.

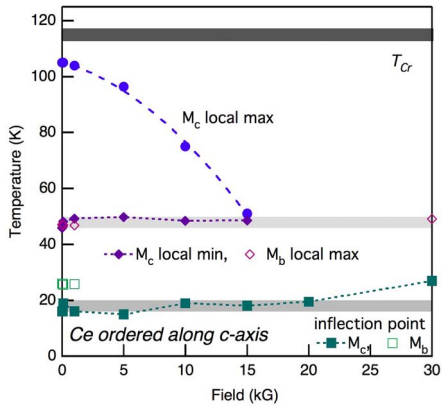

FIG. 4. (Color online) The magnetic phase diagram of $CeCrSb_3$. Open (closed) symbols represent b axis (c axis) data. The dashed line along the local maximum of M_c is a parabola, while the remaining lines are guides for the eye. The dark line at $T_{Cr}=115$ K is the ferromagnetic ordering temperature due to the Cr ions. The light gray line at 48 K indicates the start of Ce ordering, which is complete at 18 K, the bottom solid line (see Discussion).

For $T<18$ K, the resistivity falls even faster due to the reduced scattering from the Ce moments,[19] which have become ordered by this temperature, and obeys a power law $\Delta\rho=\rho(T)-\rho_0=AT^2$ [Fig. 3(b)].

IV. DISCUSSION

$CeCrSb_3$ shares many features with $LaCrSb_3$. They are isostructural, and the crystallographic anisotropy leads to unique and complex behavior. In small fields ($H<250$ G), $LaCrSb_3$ has a spin reorientation at 95 K.[4,5] Features present near zero field ($H=10$ and 20 G) for $CeCrSb_3$ suggest similar behavior. In addition, the electrical resistivity shares many features, including a change from nonmetallic ($d\rho/dT<0$) to metallic ($d\rho/dT>0$) behavior at T_{Cr} along the a axis, while metallic behavior was found for all temperatures within the plane. The electrical resistivities of both $LaCrSb_3$ and $CeCrSb_3$ were found to have a power law dependence but with different exponents. $LaCrSb_3$ varied as $T^{3/2}$ over a wide temperature range,[5] and $CeCrSb_3$ varies as T^2 for $T\lesssim 17$ K, the expected behavior for a Fermi liquid.

Just below T_{Cr}, $LaCrSb_3$ showed no magnetic anisotropy within the plane with the moments aligning in the direction of the magnetic field. However, as the temperature was lowered, a local maximum was found along the c axis due to the Cr spins preferring alignment along the b axis. The temperature at which the full magnetic anisotropy was realized decreased linearly with applied field and was fully suppressed by 3.71 kG.[5] For $CeCrSb_3$, a similar local maximum in M_c was found to decrease parabolically with field (see Fig. 4). Unlike $LaCrSb_3$, this is not suppressed to $T=0$ due to the magnetic interactions of the Ce^{3+} f electrons.

Polycrystalline measurements on the magnetization and electrical resistivity of $CeCrSb_3$ indicate an ordering of the Ce^{3+} moments at 16,[2] 30,[12] and 10 K.[20] These groups also found similar range in the value of T_{Cr}. Leonard *et al.* did not find any anomalies in the thermal expansion below T_{Cr}.[12,20] Our results on single crystals help in understanding the nature and interactions of the $3d$-$4f$ moment interactions.

First, it is clear from the isothermal magnetization measurements at 5 K that the Ce moments become aligned along the c axis. As pointed out above, the difference in the saturation magnetization between M_c and M_b is $1.99\mu_B$/f.u., which is close to the Hund's rule saturation value predicted for Ce^{3+}, $2.14\mu_B$. No evidence for a spin-flop transition was found in M_b up to 160 kG, indicating a large magnetic anisotropy at 5 K.

The intrigue arises when determining the temperature at which the Ce^{3+} moments become ordered along the c axis. The first indication of Ce^{3+} ordering appears at 48 K, the location of the maximum in M_b and the local minimum in M_c (see Figs. 1 and 4). These two features coincide and have very little field dependence. Figure 4 indicates this with the gray line at 48 K which connects the data from the local minima along the c axis with the local maxima along the b axis. The saturation magnetization along the b axis was found to be largest at $T=50$ K, and, as stated above, increasing the field up to 160 kG did not result in a further change of M_b.

The electrical resistivity points toward an ordering temperature of 18 K, as seen by the peak in $d\rho/dT$ [Fig. 3(a)]. This temperature coincides with the inflection point in the magnetization (peak in dM/dT) along the c axis at 19 K but is lower than the inflection point in M_b at 26 K (Figs. 1 and 4). The magnetization suggests a gradual alignment of the Ce^{3+} moments, starting at 48 K where M_c begins to increase, and the resistivity points toward a full alignment of the Ce^{3+} moments by 18 K, where the loss of spin scattering results in a decrease of the electrical resistivity. Figure 4 indicates the full ordering of Ce below 18 K with a solid gray line. Initial specific heat measurements support this picture because they do not indicate the presence of an anomaly below T_{Cr}, which suggests a gradual loss of magnetic entropy as the Ce moments become ordered. These observations suggest that while the easy axis for the Cr moments is along the b axis, the Ce^{3+} moments undergo a sluggish ordering between 48 and 18 K along the c axis.

V. CONCLUSION

The large crystalline anisotropy of $CeCrSb_3$ results in large anisotropy in the transport properties. $LaCrSb_3$ is an isostructural compound with no $4f$ moments, which has a ferromagnetic transition at 132 K due to the alignment of the Cr moments along the b axis. $CeCrSb_3$ adds a $4f$ moment, which interacts with the Cr $3d$ moments. Above the Curie temperature, both compounds have similar transport properties. However, the presence of the $4f$ moment begins to have dramatic effects on the system below 48 K, where the Ce moments begin to align toward the c axis. At 18 K, the alignment is complete, and the ground state of the system is one in which the $3d$ moments from the Cr ions are oriented along the b axis, just as in $LaCrSb_3$, and the $4f$ moments from the Ce^{3+} ions are aligned along the c axis.

ACKNOWLEDGMENTS

We acknowledge the help and support of both Z. Fisk and M. Torelli. We would also like to thank Julia Carmen for her insightful conversations and poignant criticism. The work at LLNL was performed under the auspices of the U.S. Department of Energy by the University of California, Lawrence Livermore National Laboratory, under Contract No. W-7405-Eng-48. D.P.Y. gratefully acknowledges support from the National Science Foundation (Grant No. DMR-0449022).

[1] M. Brylak and W. Jeitschko, Z. Naturforsch., B: Chem. Sci. **B50**, 899 (1995).
[2] K. Hartjes, W. Jeitschko, and M. Brylak, J. Magn. Magn. Mater. **173**, 109 (1997).
[3] S. J. Crerar, L. Deakin, and A. Mar, Chem. Mater. **176**, 2780 (2005).
[4] E. Granado, H. Martinho, M. S. Sercheli, P. G. Pagliuso, D. D. Jackson, M. Torelli, J. W. Lynn, C. Rettori, Z. Fisk, and S. B. Oseroff, Phys. Rev. Lett. **89**, 107204 (2002).
[5] D. D. Jackson, M. Torelli, and Z. Fisk, Phys. Rev. B **65**, 014421 (2002).
[6] W. A. MacFarlane, K. H. Chow, Z. Salman, A. V. Tkachuk, and A. Mar, Physica B **374-375**, 71 (2006).
[7] M. Richter, J. Rusz, H. Rosner, K. Koepernik, I. Opahle, U. Nitzsche, and H. Eschrig, J. Magn. Magn. Mater. **272-276**, e251 (2004).
[8] J. Shim and B. Min, J. Magn. Magn. Mater. **272-276**, e241 (2004).
[9] N. P. Raju, J. E. Greedan, M. J. Ferguson, and A. Mar, Chem. Mater. **10**, 3630 (1998).
[10] D. D. Jackson and Z. Fisk, J. Magn. Magn. Mater. **256**, 106 (2003).
[11] L. Deakin, M. J. Ferguson, and A. Mar, Chem. Mater. **13**, 1407 (2001).
[12] M. Leonard, S. Saha, and N. Ali, J. Appl. Phys. **85**, 4759 (1999).
[13] D. D. Jackson and Z. Fisk, J. Alloys Compd. **377**, 243 (2004).
[14] L. Deakin and A. Mar, Chem. Mater. **15**, 3343 (2003).
[15] I. S. Dubenko, P. Hill, and N. Ali, J. Appl. Phys. **89**, 7326 (2001).
[16] D. D. Jackson and Z. Fisk, Phys. Rev. B **73**, 024421 (2006).
[17] K. N. R. Taylor and M. I. Darby, *Physics of Rare Earth Solids* (Chapman and Hall, London, 1972).
[18] H. Zijlstra, *Experimental Methods in Magnetism* (Wiley, New York, 1967), Vol. 2, p. 127.
[19] M. Fisher and J. Langer, Phys. Rev. Lett. **20**, 665 (1968).
[20] M. Leonard, I. Dubenko, and N. Ali, J. Alloys Compd. **303-304**, 265 (2000).